23rd ABCM International Congress of Mechanical Engineering
December 6-11, 2015, Rio de Janeiro, RJ, Brazil

CURRENT FORCES ON A SUBSEA PIPELINE WITH FREE-SPAN BY USING COMPUTATIONAL FLUID DYNAMICS

Humberto Arakaki Junior
UNICAMP. Rua Mendeleyev, 200, Barão Geraldo. CEP: 13083.860 Campinas,SP, Brazil.
humberto@dep.fem.unicamp.br

Diener Volpin Ribeiro Fontoura
DPR Engenharia. Av. Dr. Romeu Tórtima, 240, sala 5, Barão Geraldo. CEP: 13084-791. Campinas, SP, Brazil.
dvolpin@dprengenharia.com

José Roberto Nunhez
UNICAMP. Av. Albert Einstein, 500, Barão Geraldo. CEP: 13083-852. Campinas,SP, Brazil.
nunhez@feq.unicamp.br

Celso Kazuyuki Morooka
UNICAMP. Rua Mendeleyev, 200, Barão Geraldo. CEP: 13083.860 Campinas,SP, Brazil.
morooka@dep.fem.unicamp.br

Abstract. *Subsea pipelines which present free span portions suffer actions from the sea current. It can result in Vortex Induced Vibration (VIV), which can damage and cause possible failure by several values for the fatigue processes. In this work, Computational Fluid Dynamics (CFD) is used to evaluate hydrodynamic current forces, in particular vortex shedding forces. Seabed effects are also investigated. A circular cross section for the pipeline with external diameter (D) is used to build two-dimensional numerical model. Simulations of the flow past the circular section nearby a plane wall are carried out for the Reynolds number around 20000. Drag and lift forces are evaluated. Gap (e) between the circular section and the wall were considered and results were tested with different turbulence models (SST and k-ε). An open source code (OpenFOAM®) and a free software (Salome) was used to create the geometry and mesh. Simulation results were compared with the literature. Results show that almost no effect from the wall is observed for e/D>1. For 1<e/D<0.5, even though vortex shedding still happen and wall effects were observed. Finally, for 0.3<e/D<0.1, vortex shedding is not observed. In general, the procedure here presented has shown good results for drag and lift forces.*

Keywords: *CFD, subsea pipeline, free span, circular cylinder, vortex shedding.*

1. INTRODUCTION

Oil and gas from offshore oil fields are transported from seabed to floating production units and oil storage terminals through risers. They are subjected to corrosion due to the external environment, internal attack of contaminants from produced oil and gas, current forces, motion of the platform due to the wave, wind and directly action of sea waves. Free span can appear throughout its length as a result of seabed unevenness, and the interaction of this portion of the pipeline with the sea current may shed vortices on the outside surface of the cylinder (riser).

Vortices can give rise to two forces: one parallel (F_D) and another one transversal (F_L) to the flow responsible for vibration on the pipe in a phenomenon known as Vortex Induced Vibration (VIV), which in turn lead to an early fatigue of the riser, reducing the expected lifetime. As shown in a previous study by numerical simulations by (Saito and Morooka, 2010), drag and lift forces increases when velocity is increasing while the values of these force coefficients decrease. Severity of the VIV on free span portion of subsea pipelines is function not only of the Reynolds number but also of the distance between pipeline to the sea bottom. If the bottom is considered as a wall (*e*), or gap ratio between the pipe and the wall is (*e/D*), where *D* is the pipeline diameter.

Many experimental studies (Bearman and Zdravkovich, 1978; Tanigushi and Miyakoshi, 1990; Price *et al.*, 2002) have been conducted in the past, regarding a cylinder close to a wall, under the incidence of a water current. One of the main conclusion of those studies is that regular vortex shedding is suppressed when the cylinder approaches the wall, at a value defined as the critical gap.

The vortex shedding usually disappears when $e/D<0.3$. Experiments conducted by (Roshko *et al.*, 1975) with $Re=2.10^4$ presented suppression of the vortex shedding for $e/D<0.2$, and the wall effect can be neglected when $e/D>1$, approximately. Suppression of the vortex shedding is associated to changes of the position of the stagnation point on the cylinder outside surface, which moves to a position closer to the wall, and the angular position of the separation point (free-stream side of the cylinder moves upstream and wall side moves downstream).

Thus vortex shedding are suppressed when cylinder is close to the wall due to the asymmetric shear layer development since the free-stream side grows larger and stronger than the opposite side. Therefore, interaction between those two vortices is highly inhibited or totally inhibited for small values of *e/D*, leading to partial or complete suppression of regular vortex shedding.

Average flow around the cylinder is asymmetric, and the average lift coefficient has non-zero values. For *e/D*=0.2-0.3, lift coefficient assumes low values increasing considerably for *e/D*<0.2 (Fredsoe and Hansen, 1987).

Two main approaches usually are available to estimate the drag and lift coefficients, respectifully, on a cylinder, and they are: (1) Computational Fluid Dynamics (CFD) and (2) semi-empirical models (Morooka *et al.*, 2006). The first one directly solves the Navier-Stokes equations, and the second one is based on experiments with risers and cylinders. As an alternative approach, CFD results can be used as an input for semi-empirical methods (Caire *et al.*, 2014) or to investigate hydroelastic problems in marine risers (Yamamoto *et al*., 2004).

In this work, computational simulations have been developed by the application of a free and open CFD source code, the OpenFOAM®. This software applies the finite volume technique to discretize the transport equations. In order to evaluate hydrodynamic current force coefficients in the cylinder close to a wall, *Re* number of 2.10^4 was chosen, and the turbulence model SST is taken for the stationary cylinder for a fixed current value. The standard solver pimpleFoam and a transient solver for incompressible flow by using the PIMPLE algorithm have been employed.

2. NUMERICAL METHOD

Vortex shedding is a function of Reynolds number as in Eq. (1) and the frequency is proportional to the cylinder diameter and the incoming flow velocity (*U*) as in Eq. (2):

$$Re = \frac{DU}{\nu} \tag{1}$$

$$St = \frac{f_s D}{U} \tag{2}$$

where, ν is the kinematic viscosity, f_s the vortex shedding frequency and *St* is the Strouhal number, which is approximately 0.2 for fixed and isolated cylinders in the range $10^3<Re<10^5$.

Lift force oscillates according to the vortex shedding frequency. The drag coefficient oscillates each time a vortex is shed from one side to another in the perpendicular direction of the current, from outside the surface of the stationary cylinder. Therefore, the frequency of the drag force is twice the lift force for stationary cylinders. Mean drag and lift coefficients are defined by Eqs. (3) and (4):

$$\bar{C}_D = \frac{\bar{F}_D}{(1/2)\rho D U^2} \tag{3}$$

$$\bar{C}_L = \frac{\bar{F}_L}{(1/2)\rho D U^2} \tag{4}$$

in which, ρ=fluid density, $\bar{F}_D$ and $\bar{F}_L$ are mean drag and lift forces, respectively.

As a general rule the coefficient value decreases when the gap ratio decreases. Several experimental results found that $\bar{C}_D$ increases with the increasing of the ratio *e/D*, but only up to a certain value and remains constant for higher values of *e/D*.

This behavior is associated with boundary layer thickness of the incoming flow (Zdravkovich, 1985). When cylinder is totally under potential flow $\bar{C}_D$ assumes constant value.

In this study, the thickness of the boundary layer (δ) over the flat wall without considering the cylinder is estimated by simulating the flow without the cylinder. A value at the order of δ/D=0.01 was obtained.

Average flow around the cylinder is asymmetric leading to a non-zero mean lift force. Average pressure distribution around the cylinder is symmetric when *e/D*=1, which means that lift is negligible. This symmetry disappears when *e/D*=0.1 or 0, resulting in non-zero mean lift coefficient and directed outwards the wall (Sumer and Fredsøe, 2006).

The pressure distribution also shows that when *e/D* is reduced, there is a mean force acting on the cylinder repelling it from the wall and this force decreases very rapidly when the cylinder is moved away from the wall, as observed by (Roshko *et al.*, 1975).

2.1 Equations of motion

The governing equations for a Newtonian, incompressible viscous flow in two-dimensions are the conservation of mass and momentum (Navier-Stokes equations):

$$\frac{\partial u_i}{\partial x_i} = 0 \qquad i = 1,2 \tag{5}$$

$$\rho\frac{\partial u_i}{\partial t} + \rho\frac{\partial u_i u_j}{\partial x_j} = -\frac{\partial p}{\partial x_i} + \mu\frac{\partial^2 u_i}{\partial x_j \partial x_j} \tag{6}$$

in which, u_i are the velocity components in x and y directions.

When using a turbulence model, the Navier-Stokes equations are replaced by RANS (Reynolds Averaged Navier-Stokes) equations. In order to obtain the RANS equations, instantaneous properties are split up into a mean (time-averaged) component and a fluctuating component, as in eq. (7):

$$u_i = \bar{u}_i + u_i' \tag{7}$$

Where $\bar{u}_i$ is the time-averaged component and u_i' the fluctuating component.

Replacing the instantaneous properties in the Navier-Stokes equations, results in RANS equations:

$$\rho\frac{\partial \bar{u}_i}{\partial t} + \rho\frac{\partial \bar{u}_i \bar{u}_j}{\partial x_j} = -\frac{\partial \bar{p}}{\partial x_i} + \frac{\partial}{\partial x_j}\left(\mu\frac{\partial \bar{u}_i}{\partial x_j} + \overline{\rho u_i' u_j'}\right) \tag{8}$$

Where, the term $\overline{\rho u_i' u_j'}$ is referred as the Reynolds stress tensor and represents an additional stress tensor due to fluctuating velocities. In order to numerically solve the equations above the Reynolds stress tensor has to be approximated by a model.

2.2 Turbulence model

Turbulence model, mesh generation and the algorithm to solve the equations are essentially the main parameters in a CFD program. Although there is not a universal turbulence model that can solve all possible flow conditions, several researches have been made an effort to assess the most appropriate model for a specific situation.

The k-ω and k-ε models are common turbulence models in CFD simulations. These two equations models provide not only computation of *k* (kinetic energy of turbulent fluctuations) but also for the turbulence length scale. Consequently, two-equations models can be used to predict properties of a given turbulent flow (Wilcox, 1994)

In industrial applications the k-ε model is commonly used due to a good convergence rate and relatively low memory requirement but when flow fields exhibits adverse pressure gradients this model is not accurate. The k-ω model is similar but uses wall functions and has more difficult convergence. Equation of ω can be solved in viscous sublayer without stability problems as in the case of the ε equation, so k-ω model performs better when accuracy near wall is needed (Saltara and Pedrão, 2012). Nguyen and Temarel (2014) evaluated different models for a stationary cylinder for different values of Re (3900 and 10000) and concluded that k-ε model has a good agreement for the lift coefficient when Re=3900 and the k-ω model for the drag coefficient when $Re=10^4$.

The model chosen for these simulations was the SST, implemented in OpenFOAM® and developed by (Menter, 1994). This model is a combination of the k-ε in the free stream and the k-ω near walls and has proved to be a good turbulence model for flows with adverse pressure gradients. The maximum y^+ value (distance from the wall to the centre of the first cell) recommended for this turbulence model must be around two, and all the simulations were carried out in compliance with this value.

Approximations of the initial parameters for this model are required in order to perform the numerical investigation, such as turbulent kinetic energy (k), dissipation rate of specific turbulence (ω) and dissipation rate of turbulence (ε).

$$k = \frac{3}{2}(UI)^2 \tag{9}$$

$$\omega = \frac{\sqrt{k}}{l} \tag{10}$$

$$\varepsilon = C_\mu \frac{k^{3/2}}{l} \tag{11}$$

in which, I (=0.05) is the turbulence intensity, l (=0.007D)is the turbulence length scale and C_μ (=0.09) is a constant of the model (Silva *et al.*, 2013).

2.3 Geometry, mesh and boundary conditions

Figure 1 presents the computational domain with e ranging from 0.1D to 3D to assess the wall effect and dimensions in x, y and z axis are 34D, 14D and 0.1D respectively. The diameter was 0.0635m, ρ=996 kg/m³ and μ=10^{-3} Ns/m².

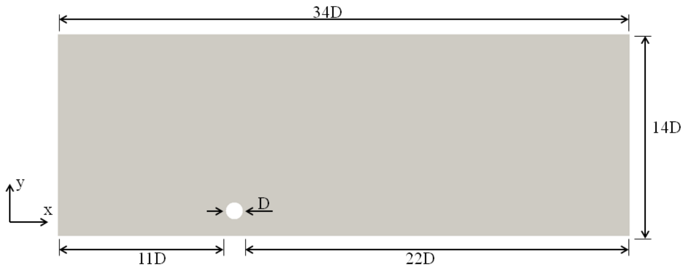

Figure 1. Computational domain.

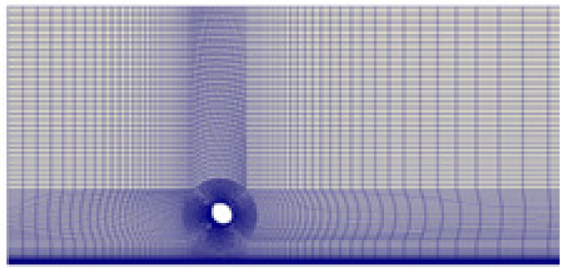

Figure 2. Refinement near wall and cylinder.

The dimensions were chosen so that the top, inlet and outlet have no influence in the region of interest. Computations are performed only in axis x and y due to the high computational costs associated with the tri-dimensional case.

Inlet velocity (axis x) is set to U=0.315m/s (Re=2.10^4), and outlet pressure specified is set to zero.

A fine mesh with tetrahedrals was employed in order to obtain a high resolution at the boundary layer. Seabed and riser are represented as simple geometries (rectangular for the seabed and a circle for the riser). To this end, the free software Salome® is chosen, so mesh can be created and exported to OpenFOAM®.

The O-type grid around cylinder is employed, to avoid element distortion. In the boundary layer area hexaedrical elements with a growth gradient were employed for a proper discretization, as represented in Fig. 2.

A key issue to determine numerical accuracy is the grid insensitivity (mesh independence) of the results and the most common way to assure grid independence is to repeat the computation on a grid with twice as many grid points. The mesh independence study was realized comparing the values of mean drag for each mesh density.

3. RESULTS

3.1 Mesh generation and grid independence

Several grids were made and the mesh independence test was carried out, with a maximum y^+ value of 2 near wall and cylinder. When the gap ratio decreases, the distance between cylinder and the bottom of the domain (wall) also decrease and the cells became smaller, reducing y^+ value as presented in Figure 4, summarizing some simulation cases. The number of volumes or cells also increased when a more refined mesh was required. Figure 3 presents the grid independence test.

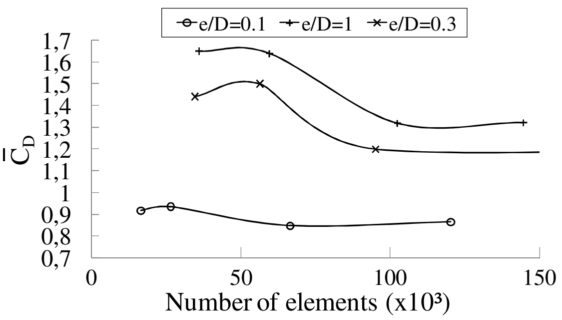

Figure 3. Grid independence.

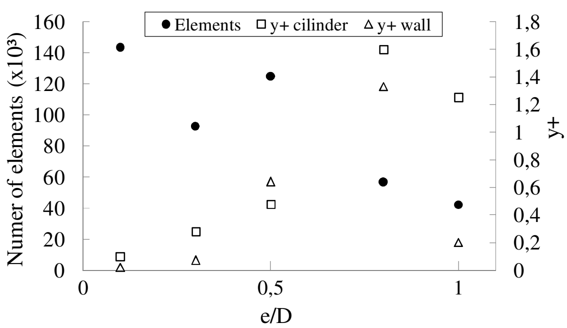

Figure 4. Number of elements and y^+ values.

3.2 Comparison of the different turbulence models used.

Simulations were carried out using two turbulence models (SST and standard k-ε) and the same initial conditions for different gap ratios: 0.3, 0.5, 0.8 and 1.

The results for the mean drag and lift coefficients were compared with experimental data extracted from plots of (Roshko *et al.,* 1975) and are summarized in Tab. 1. Values for mean drag in SST model are closer and apparently followed the pattern of the experimental curve unlike the k-ε model. For the lift coefficient, both models presented similar results.

Considering an initial estimative from these results, all of the following simulations were carried out using the turbulence model SST. The SST model properly solves flows with adverse gradient pressure and is a hybrid between k-ε and k-ω models, minimizing the deficiencies of both models. It essentially uses the k-ω model in near wall regions and k-ε model in free shear flows.

Table 1. Comparison of turbulence models with (Roshko *et al.,* 1975).

e/D	k-ε				SST				(Roshko *et al.,* 1975)	
		Error (%)		Error (%)		Error (%)		Error (%)		
0.3	0.96	13	0.23	4.5	1.14	3.6	0.32	45	1.1	0.22
0.5	0.96	20	0.12	33	1.2	0	0.15	17	1.2	0.18
0.8	0.79	38	0.04	60	1.31	3	0.10	0	1.27	0.10
1	0.82	35	0.06	0	1.32	4.7	0.09	50	1.26	0.06

3.3 Drag and lift in a turbulent flow with *Re*=2.10^4 for different values of *e/D*.

Simulations using OpenFOAM® were carried out in the range 0.1<*e/D*<3. Results for mean force coefficients were considered taking the average of time-history values of drag and lift coefficients and compared with experimental data.

- *e/D*=1, 2 and 3.

The flow in this range of *e/D* represents the same flow as an isolated cylinder. At ratios *e/D*>1, the vortex shedding occurs due to the alternate interaction between the shear layers around the cylinder. Also, the vortex wake also occurs as expected for this flow. In these cases there is not wall effect on the cylinder, as experimentally verified by (Roshko *et al.,* 1975). In accordance with experimental results from several authors and the simulations, the case *e/D*=1 presented the same behavior as the cases *e/D*=2 and *e/D*=3. Thus only velocity magnitude contours and time history of drag and lift coefficients for *e/D*=1 are represented in Fig. 5 and Fig. 6.

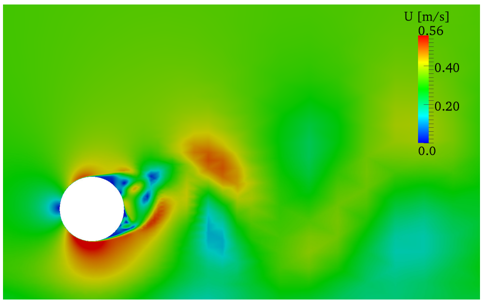

Figure 5. Flow visualization for *e/D*=1.

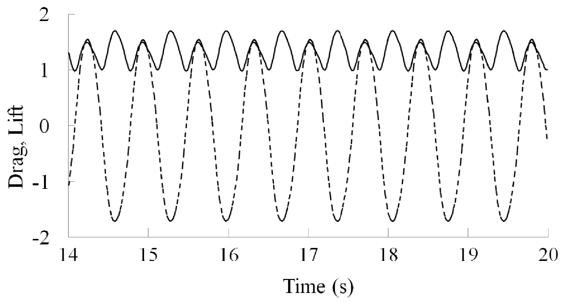

Figure 6. Time history of drag (continuous line) and lift (dashed line) for *e/D*=1.

- *e/D*=0.8

When *e/D*<1, the wall may influence the flow around the cylinder, decreasing the value of the drag and increasing lift. These results are very close to the previous one. Again, the dominant frequency of the drag is twice the lift, as expected. Figure 7 and Fig. 8 are the velocity magnitude contour and time history of the drag and lift coefficients. Likewise, the alternating vortex wake may be seen in this flow as in the previous case.

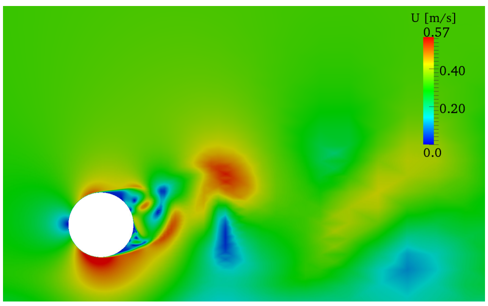

Figure 7. Flow visualization for *e/D*=0.8.

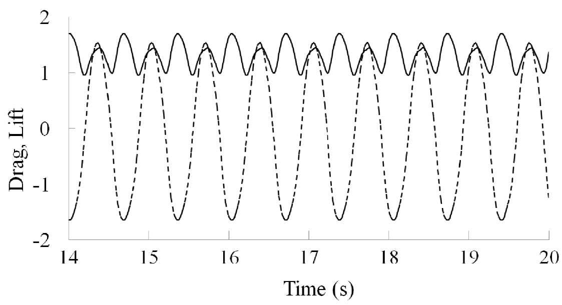

Figure 8. Time history of drag (continuous line) and lift (dashed line) for *e/D*=0.8.

- *e/D*=0.5

Vortex shedding is not suppressed for this gap ratio. The wall side shear layer is less developed than the other side leading to a weaker interaction between the layers as the distance from the wall decreases. Figure 9 is the velocity magnitude contour and Fig. 10 presents the time history of drag and lift coefficients.

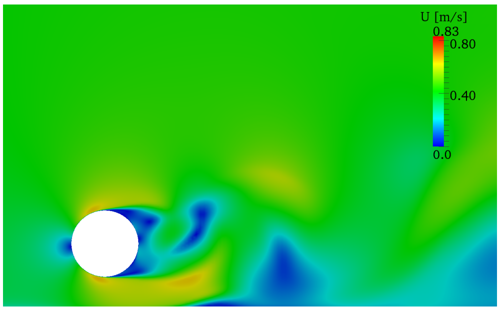

Figure 9. Flow visualization for *e/D*=0.5.

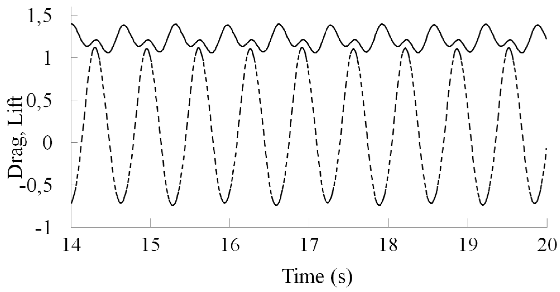

Figure 10. Time history of drag (continuous line) and lift (dashed line) for *e/D*=0.5.

- *e/D*=0.3

The boundary layer of the lower face of the cylinder and that of the flat wall interact with each other, suppressing the vortex shedding at the near wall side. The frequency for the drag and the lift are the same. There is a separation region upstream the cylinder, as experimentally observed by (Price *et al.*, 2002) for the gap ratio of *e/D*=0.25 and 0.375. Figure 11 is the velocity magnitude contour and Fig. 12 is the time history of the drag and lift coefficients.

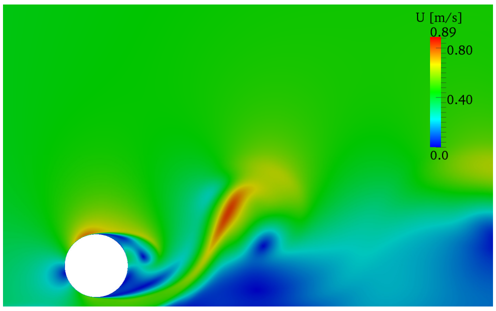

Figure 11. Flow visualization for *e/D*=0.3.

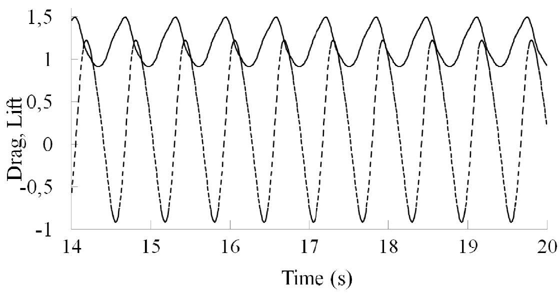

Figure 12. Time history of drag (continuous line) and lift (dashed line) for *e/D*=0.3.

- *e/D*=0.1

The interaction between the layers ceases to exist and vortex shedding is suppressed. Figure 13 is the velocity contour plot and indicates that vortex shedding is suppressed and there is almost no flow below the cylinder, creating a large vortex upstream the cylinder, as noticed by (Price *et al.*, 2002). When the pipe is placed at the seabed the length of the wake is around six times the cylinder diameter, according to studies from (Bearman and Zdravkovich, 1978) for $Re=4.8.10^4$. In this study, a wake of around 12*D* was obtained. Many factors may contribute to the difference between the reported experimental wake value and the simulated one. For sure, the Reynolds number contribute to the difference between experimental and simulated values. Figure 14 is the time-history of the drag and lift. The drag and lift tend to a constant value in accordance with the suppressing of the vortex shedding.

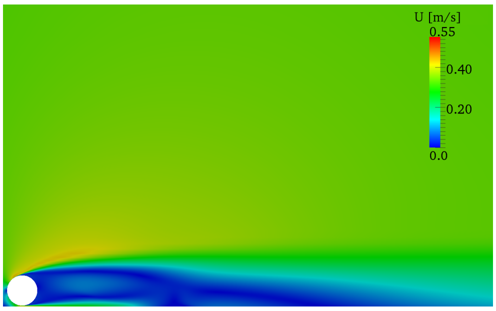

Figure 13. Flow visualization for *e/D*=0.1.

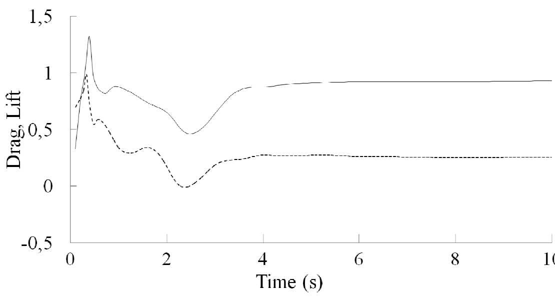

Figure 14. Time history of drag (continuous line) and lift (dashed line) for *e/D*=0.1.

Figures 15 and 16 summarize the results simulated with the OpenFOAM® software for the drag and lift coefficients, both for the same Reynolds number. The results agree well with experimental data from (Roshko *et al.*, 1975). Values of the mean lift coefficient are slightly higher than the experimental data. This overestimation is expected for a 2D turbulent flow around a cylinder (Neto, 2012). Turbulence parameters may also contribute for these deviations.

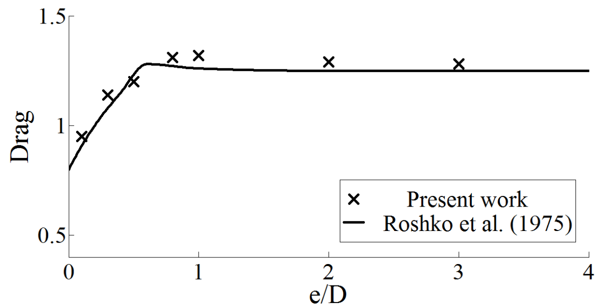

Figure 15. Results for mean drag coefficient and comparison with (Roshko *et al.*, 1975)

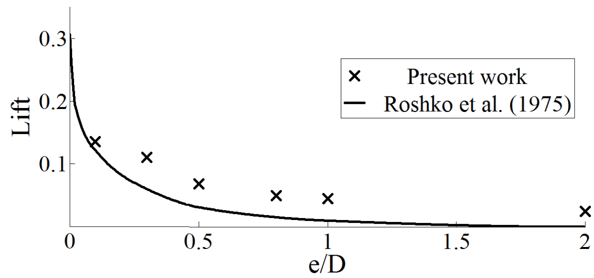

Figure 16. Results for lift coefficient and comparison with (Roshko *et al.*, 1975)

3.4 Strouhal number

The vortex shedding frequency is determined by time history of the lift using the algorithm of Fast Fourier Transformation (FFT). The dominant frequency of the drag is twice the lift and the peak point of the lift frequency is the vortex shedding frequency. Figures 17 and 18 show the FFT of the drag and the lift coefficients for the cases of *e/D*=1 and *e/D*=0.3.The cases 3<*e/D*<0.5 presented the same behavior as *e/D*=1, except for the values of the peaks. With the decreasing of *e/D*, the value of the peak decreased, indicating that shedding becomes weaker as the gap ratio decreases, as experimentally observed by (Lei *et al.,* 1999).

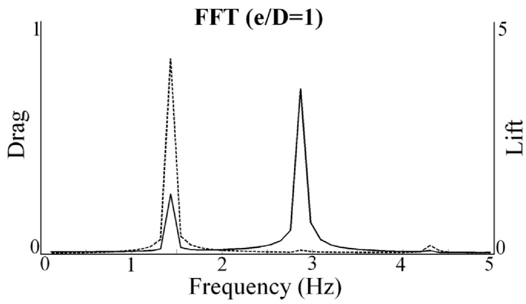

Figure 17. FFT of drag (continuous line) and lift (dashed line) for *e/D*=1.

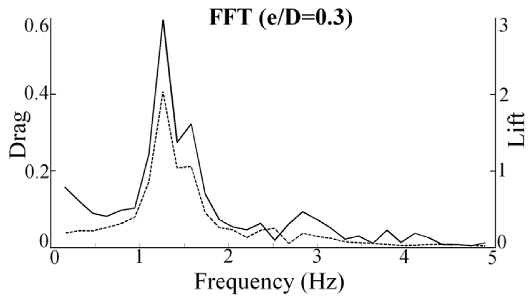

Figure 18. FFT of drag (continuous line) and lift (dashed line) for *e/D*=0.3.

The simulated values of the Strouhal number (*St*) were 0.28 for *e/D*=1 and 0.25 for *e/D*=0.3, which follows the observation of (Bearman and Zdravkovich, 1978). They observed that *St* is constant for *e/D*>0.3 and decreases for *e/D*<0.3. Further investigation for gaps lower than 0.3 would be needed to confirm their observation.

4. CONCLUSIONS

Computational fluid dynamics was used in this work to evaluate the force coefficients in a circular cylinder near a plane wall. Time dependent drag and lift were obtained and compared with available experimental data in the literature. A free and open source code (OpenFOAM®) was employed.

From the results, the mesh grid has a greater influence on the calculations, especially in regions around the cylinder surface and neaby the bottom of the domain. Simulations were carried out in a thin boundary layer over the plane wall, so the gap ratio, rather than the thickness of the boundary layer has influence on the force coefficients. This agrees with results in the literature (Huang and Larsen, 2010).

The simulated results indicated that the SST turbulence model is more suitable than the k-ε model for it better represented both the drag and lift coefficient.

OpenFOAM® predicted with accuracy the force coefficients (hydrodynamic forces) of subsea pipelines. Observation of the velocity contours plot helped to better understand experimental results such as these by (Bearman and Zdravkovich, 1978) and (Price *et al.,* 2002).

5. ACKNOWLEDGEMENTS

Authors acknowledge the following sponsors: National Agency of Petroleum, Natural Gas and Biofuels (ANP), Financial Agency for Studies and Projects (FINEP) and Ministry of Science, Technology and Innovation (MCTI) through the PRH-ANP/MCTI, Frade Japan Petroleum Limited (FJPL - a joint venture established by INPEX Corporation and Sojitz Corporation), FUSP, and Petrobras for the financial support.

6. REFERENCES

BEARMAN, P.W., ZDRAVKOVICH, M.M., 1978. "Flow around a circular cylinder near a plane boundary". *Journal of Fluid Mechanics*, Vol. 89, p. 33-47.

CAIRE, M., NÓBREGA, P. H. A., KHALIL, R. V., 2014. "Two-dimensional numerical simulation of an oscillating cylinder in turbulent flow: comparison to experimental results". In *Proceedings of the 25th National Congress on Maritime Transportation, Ship and Offshore Construction – SOBENA 2014.* Rio de Janeiro, Brazil.

FREDSØE, J., HANSEN, E., 1987. "Lift forces on pipelines in steady flow". *Journal of Waterway, Port, Coastal and Ocean Eng*., Vol. 113, p. 139-155.

HUANG, Z., LARSEN, C. M., 2010. "Large Eddy Simulation of an oscillating cylinder close to a wall", In *Proceedings of the 29th International Conference on Ocean, Offshore and Artic Engineering* - *OMAE 2010.* Shanghai, China.

LEI, C., CHENG, L. KAVANAGH, K., 1999. "Re-examination of the effect of a plane boundary on force and vortex shedding of a circular cylinder". *Journal of Wind Engineering and Industrial Aerodynamics*, Vol. 80, p. 263-286.

MENTER, F. R., 1994. "Two-equation eddy-viscosity turbulence models for engineering applications", *AIAA Journal*, Vol. 32, p. 1598-1605.

MOROOKA, C. K., IDEHARA, A. Y., MATT, C. G. C., 2006. "Behavior of a pipeline with free span under steady current". In *Proceedings of the Ibero-Latin American Congress on Computational Methods in Engineering - XXVII CILAMCE.* Belém, Brazil.

NETO, M. C., 2012. *Simulação numérica bidimensional do escoamento ao redor de um cilindro circular próximo a uma placa plana*. MSc dissertation, Federal University of Rio de Janeiro, Rio de Janeiro.

NGUYEN, L.T.T., TEMAREL, P., 2014. "Numerical simulation of an oscillating cylinder in cross-flow at a Re number of 10.000: forced and free oscillations". In *Proceedings of the 33rdInternational Conference on Ocean, Offshore and Artic Engineering – OMAE 2014.* San Francisco, USA.

PRICE, S.J., SUMNER, D., SMITH, J.G., LEONG, K., PAIDOUSSIS, M.P., 2002. "Flow visualization around a circular cylinder near to a plane wall". *Journal of Fluids and Structures*, Vol. 16, p. 175-191.

ROSHKO, A., STEINOLFSON, A., CHATTOORGOON, V., 1975. "Flow forces on a cylinder near a wall or near another cylinder", In *Proceedings of the 2nd US Conf. Wind Engineering Research*. Colorado, USA.

SAITO, J. S., MOROOKA, C. K., 2010. "Simulação computacional do escoamento em torno de uma seção de um duto submarino". In *Proceedings of the VI Congresso Nacional de Engenharia Mecânica – CONEM 2010*. Paraíba, Brazil.

SALTARA, F., PEDRÃO, N., 2012. "Comparação entre simulações LES e URANS para escoamentos ao redor de corpos rombudos". In *Proceedings of the 8^{a} Escola de Primavera de Transição e Turbulência – EPTT 2012*. São Paulo, Brazil.

SILVA, J. V., GUERRA, D. R. S., PICANÇO, H. P., 2013. "Numerical investigation of vortex shedding on marine risers". In *Proceedings of the 22nd International Congress of Mechanical Engineering – COBEM 2013*, Ribeirão Preto, Brazil.

SUMER, B.M., FRESØE, J., 2006. *Hydrodynamics Around Cylindrical Structures*. World Scientific Publishing Co. Pte. Ltd., Singapure, Revised edition.

TANIGUSHI, S., MIYAKOSHI,K., 1990."Fluctuating fluid forces acting on a circular cylinder and interference with a plane wall". *Experiments in Fluids*, Vol. 9, p. 197-204.

WILCOX, D. C., 1994. *Turbulence Modeling for CFD.* DCW Industries, Inc., California, 1st edition.

YAMAMOTO, C. T., MENEGHINI, J. R., SALTARA, F., FREGONESI, R.A., FERRARI JR, J. A., 2004. "Numerical simulations of vortex induced vibration on flexible cylinder". *Journal of Fluids and Structures*, Vol. 19, p.467-489.

ZDRAVKOVICH, M.M., 1985. "Forces on a cylinder near a plane wall", *Applied Ocean Research*, Vol. 7, p. 197-201.

7. RESPONSIBILITY NOTICE

The authors are the only responsible for the printed material included in this paper.